Nano World Journal

https://doi.org/10.17756/nwj.2023-s5-069

Research Article

Open Access

Computational Analysis on the Structural and Spectroscopic Properties of Natural Compound Curcumin and its Interaction with Nanometric Bacterial Porins

Vandana Kumari[1], Priyanka Kumari[1], Amrita Biswas[1], Saikat Chattopadhyay[2] and Susruta Samanta[1*]

[1]*Department of Chemistry, Manipal University Jaipur, Rajasthan, India*

[2]*Department of Physics, Manipal University Jaipur, Rajasthan, India*

***Correspondence to:**
Susruta Samanta
Department of Chemistry,
Manipal University
Jaipur, Rajasthan, India.
E-mail: susruta.samanta@jaipur.manipal.edu

Received: October 20, 2023
Accepted: December 21, 2023
Published: December 27, 2023

Citation: Kumari V, Kumari P, Biswas A, Chattopadhyay S, Samanta S. 2023. Computational Analysis on the Structural and Spectroscopic Properties of Natural Compound Curcumin and its Interaction with Nanometric Bacterial Porins. *NanoWorld J* 9(S5): S396-S402.

Published by United Scientific Group

Abstract

Natural molecules with biological activities, for example, antibacterial, antioxidant, anti-carcinogenic, and anti-inflammatory properties are an interesting area for study. We have focused on the naturally occurring molecule - curcumin to study its properties and interaction with bacterial proteins. We have employed a hybrid computational approach to study the interactions at a molecular level. The molecular structure of curcumin was optimized using quantum mechanical methods. The validity of the model was verified using a comparative structural analysis of the keto and enol forms of curcumin and by studying the spectra of their relevant structural isomers. Interaction of curcumin with the bacterial porins of the Gram-negative bacteria was studied using molecular docking analysis. The most expressed outer membrane porins of two different classes - OccK and OccD of *Pseudomonas aeruginosa* were selected as they are the major points of entry for antibiotic molecules to the bacterial cell. We have identified the affinity sites inside the porins. Our study shows that the similarity in the chemical environment inside the porins plays a crucial role in targeted movement of the curcumin molecule.

Keywords

Curcumin, Bacterial porin, Natural molecule, Antibiotics

Introduction

Turmeric (*Curcuma longa*) belongs to the curcuminoid family and has been utilized for ages in traditional therapies as well as dietary spices [1] (Figure 1). Turmeric contains the active substance curcumin, which has three major variations in its structure: curcumin, demethoxycurcumin, and bisdemethoxycurcumin (Figure 2). Among these, the native structure of curcumin has been well researched for its properties [2-5]. Curcumin has been shown in numerous studies to exhibit a variety of biological and pharmacological activities, including anti-inflammatory, antioxidant, antioxidizing, antibacterial, anti-protozoal, anti-microbial, anti-malarial, anti-inflammatory, anti-proliferative, anti-angiogenic, anti-tumor, and anti-aging properties [6-8]. It also has the potential to be used as a therapeutic agent for wound healing, diabetes, Alzheimer disease, Parkinson disease, cardiovascular disease, pulmonary disease, and arthritis.

Curcumin has three important functional parts in its structure: an aromatic methoxy phenolic group; α, β-unsaturated β-diketo and keto-enol tautomerism (Figure 1) [9]. Curcumin could scavenge active oxygen or nitrogen-free radicals which is responsible for the activity of curcumin [10-14]. The antioxidant activity of curcumin is attributed to the phenolic -OH group, and it has been established by pulse radiolysis and other biochemical methods [13-16]. Some other studies show that this antioxidant activity of curcumin is due to the hydrogen abstraction

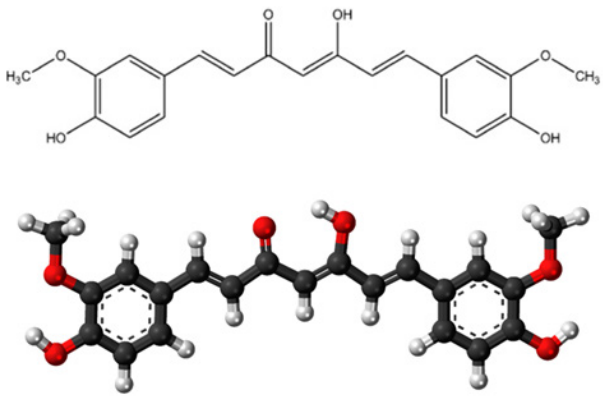

Figure 1: Chemical structure and optimized 3D structure of curcumin.

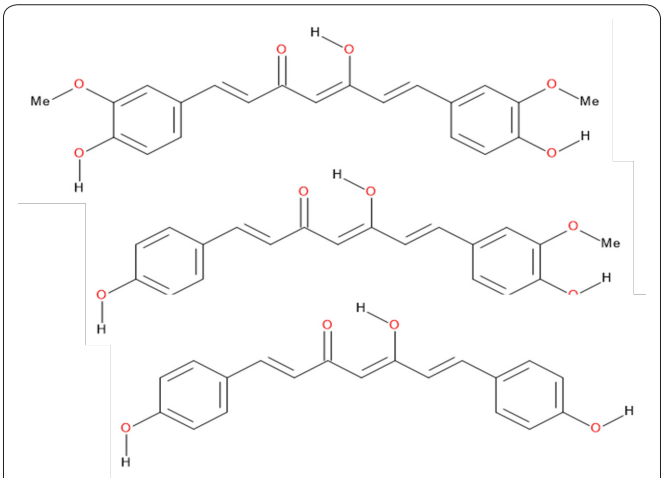

Figure 2: Structures of curcumin, demethoxycurcumin, and bisdemethoxycurcumin.

from the methylene group [17, 18]. Later, the quantum chemical study confirms that the biological activity of curcumin is due to the phenolic -OH group [15]. To a complete understanding of its biological properties, it is necessary to characterize the most stable geometrical isomers of curcumin and the factors that contributed to their relative stability.

Based on quantum mechanical calculations, and the detailed structural analysis of the diketo and enol forms of curcumin and their infrared and Raman spectra of relevant structural isomers, it has been found that enol form of curcumin is more stable than diketo form and it shows better bioactivity [4, 19, 20].

We used the model of curcumin to study its interaction with two outer membrane proteins of *P. aeruginosa* – OccD1/OprD and OccK1/OpdK. These proteins are found in the outer membrane of the bacteria, and they serve as entry points for polar molecules into the cell of bacteria [21-24]. Among these porins, OccD1 has been proven to favor positively charged molecules and OccK1 has been established to favor negatively charged molecules [25-28]. The polarity and electrostatic distribution of residues inside the channel has been proven to be a key factor in binding of polar molecules inside these channels [21, 23, 29, 30].

Though the properties of these channels as well as the antibiotic properties of curcumin have been extensively studied, there are no studies which explore the possibility of finding an interaction site of curcumin in these channels. Here, we have focused on that and computationally investigated the affinity sites of curcumin in the most expressed porins of both families to establish the validity of the proposed model of curcumin.

Methodology

Quantum mechanical calculations

We used Density Functional Theory (DFT), Hartee-Fock (HF), and Restricted Hartee Fock (RHF) to optimize the structure of curcumin and study its spectral properties. We did a comparative structural analysis of the enol form of curcumin and predicted the infrared and Raman spectra of their relevant structural isomers. These results were then used to interpret the observed vibrational spectra for the curcumin to correlate the structure with the biological activity.

We used the Gaussian 09W program to perform the quantum mechanical calculations [31]. Based on the results obtained by using different theories, DFT (with B3LYP method) with 6-31++G (d, p) basis set gives the best result with minimum energy value indicating maximum stability of the structure.

We calculated several parameters, for example, the energy distribution from HOMO-LUMO (Highest Occupied Molecular Orbital and Lowest Unoccupied Molecular Orbital), Electrostatic Surface Potential (ESP), Fourier transform infrared (FTIR) and Raman spectra, and Mulliken atomic charges. These properties were analyzed by the Gauss View software [32].

Molecular docking analysis

Molecular docking has become a fundamental technique in the drug discovery process [33-35]. Here, we describe a thorough assessment of the molecular interactions of curcumin with Gram-negative bacteria proteins using molecular docking methods. We can define the behavior of molecules at the binding site of target proteins by using the molecular docking approach to determine the interaction between the curcumin molecule and a variety of proteins at the atomic level.

The RCSB Protein Data Bank (PDB) (www.rcsb.org), was used to obtain the 3D structures of all potential targets for the Gram-negative bacteria proteins. We focused our study on two proteins: OccD1 or OprD (PDB code: 3SY7) and OccK1 or OpdK (PDB code: 3SYS). UCSF Chimera 1.11.2 was used to construct the protein structures [36].

We optimized the model of the curcumin molecule used in this study (chemical structure shown in figure 1) using DFT method. Because of its chemical makeup and abilities, curcumin can bind to specific proteins. We prepared the ligand structures for each target macromolecules using VMD [37]. We separated them from the protein, water molecules, and other byproducts to ensure unbiased binding. We used these acquired conformations as starting conformations for our docking analysis. We used Autodock4 for the docking analysis [38]. We obtained a population of potential ligand conforma-

tions and orientations at the binding site. We used PyRx program for further analysis [39]. After the docking search was finished, we selected the optimal conformation with the lowest binding energy and used Discovery Studio Visualizer to examine the interactions between complicated protein-ligand conformations, including hydrogen bonds and bond lengths.

The docking methods and parameters were validated by redocking experiment to make sure that the docking studies were legitimate and accurately represented the prospective binding model. To test the Autodock program's ability to replicate the orientation and position of the ligand as shown in the crystal structure, each copy of the native ligand was docked into the native protein. Success is commonly defined as having an all-atom root mean square deviation of less than 2Å between the docked location and the crystallographically observed binding position of the ligand, which we confirmed in our study.

Results and Discussion

Structure of curcumin

The chemical name for curcumin is 1,7-bis(4-hydroxy-3-methoxyphenol)1,6-heptadiene-3,5-dione, and its molecular formula is $C_{21}H_{20}O_6$. It has two ferulic acid residues connected by a methylene bridge as shown in figure 1. Both theoretical and experimental investigations demonstrated that curcumin exhibits three acidity constants for two phenolic -OH groups and one enolic -OH group. The two phenolic protons' pKa values range from 8.5 to 10.7, and the most acidic of these three is the enolic proton (pKa value 8.5) [40]. Additionally, it has been demonstrated that curcumin's antioxidant action depends on the enolic -OH group [17, 18]. Curcumin can adopt a variety of conformations which are ideal for optimizing hydrophobic interactions with the protein to which it is attached. Curcumin's phenyl rings can engage in van der Waals interactions with the side chains of the aromatic amino acids. The phenolic and carbonyl groups, which are found on the ends and in the middle of the molecule, can engage in hydrogen bonding interactions with the target macromolecules. To increase the favorable free energies of association, this structure demonstrates an efficient and focused electrostatic interaction [1].

HOMO-LUMO analysis

On the detailed analysis it was observed that curcumin shows both nucleophilic and electrophilic nature. The HOMO-LUMO energies have been determined at B3LYP/6-311++G (d, p) level. The excited-state energy of a molecule implicates the disparity between HOMO-LUMO (Figure 3) [41]. These energy values were used to calculate various physical parameters and to compare their reported values to establish usability of the present model [42-44].

We have calculated energy values of the HOMO and LUMO which resulted in an energy gap of 0.11890 eV. We used these values to calculate chemical potential (μ), chemical hardness (η), chemical softness (S), electronegativity (χ), electrophilicity, ionization energy (IE), and electron affinity (EA).

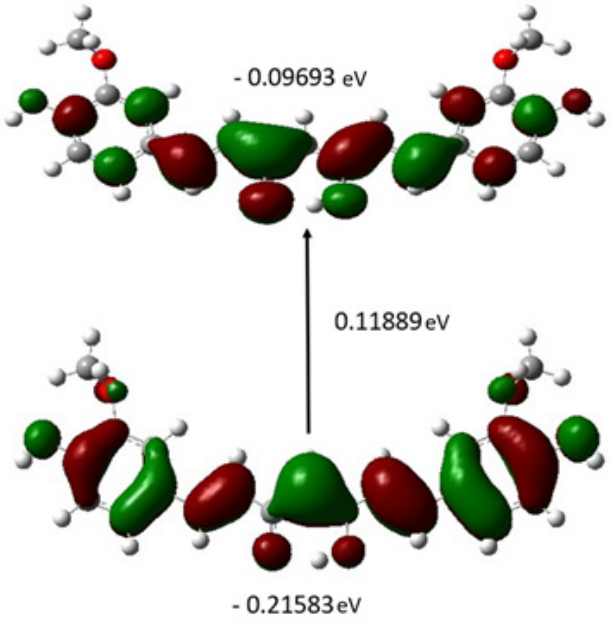

Figure 3: Energy values and energy gap between HOMO and LUMO for curcumin.

Table 1: Energy values of HOMO-LUMO and calculated parameters.

Molecular parameters	Energy (eV)
E_{homo}	-0.21583
E_{lumo}	-0.09693
E_{gap}	0.11890
$\mu = \frac{1}{2}(E_l + E_h)$	-0.15638
$\eta = \frac{1}{2}(E_l - E_h)$	-0.05944
$S = \frac{1}{2}\eta$	-0.02972
$\chi = -\mu - \frac{1}{2}(E_l + E_h)$	0.15638
$\omega = \frac{\mu^2}{2\eta}$	-0.20568
IE	0.21583
EA	0.09693

These values have been tabulated in table 1 along with the formulae used to calculate them.

ESP analysis

The ESP diagram shows the sites for nucleophilic and electrophilic properties [45, 46]. The ESP expresses the shape,

size, reactive site, and charge density of the molecule. The ESP of curcumin molecule was determined by using the B3LYP functional employing 6-311++G (d, p) level of theory and has a grid range between -7.563 x 10^2 eV to 7.563 x 10^2 eV. The ESP surface for the curcumin molecule is represented in figure 4. In the ESP map, the negative region is more concentrated around the oxygen atoms, and it is supported by the Mulliken charges. The changes on the atoms are shown in table 2. These results indicate the binding site of the curcumin molecule may lie at the electrophilic sites.

Vibrational analysis

The vibrational spectra of curcumin have been concluded with potential energy distribution analysis. The curcumin molecule has 47 atoms, which results in 135 modes of vibrations. The spectral calculation of the FTIR and Raman spectra is shown in figure 5.

The measured and interpreted experimental vibrational spectra of the curcumin molecule is the strong band at 1628 cm^{-1} and has a stretching frequency of C=C and C=O character. Most of the bands in the frequency region 1450 - 1300 cm^{-1} are highly mixed. The bands at 1290 and 1282 cm^{-1} belong to the pure in-plane C-H vibrations of the aromatic rings. The bands in 1277 - 1188 cm^{-1} are attributed to the vibration of the phenyl rings. Deformation vibrations of the two methyl groups are pure. These were observed at 1460 - 1430

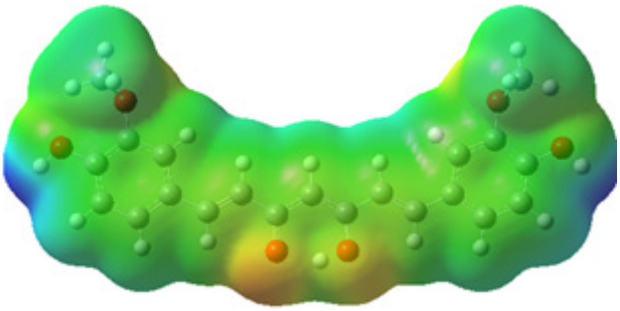

Figure 4: ESP diagram of curcumin. The maximum electrophilic reactivity is shown in red and yellow. The maximum nucleophilic reactivity is shown in blue. The neutral region is shown by green.

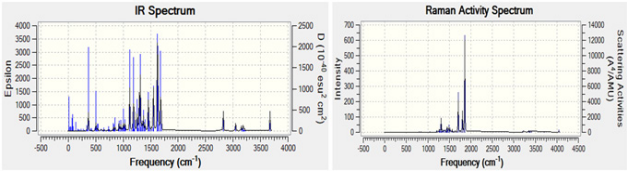

Figure 5: Computed FTIR and Raman spectra of the curcumin molecule.

Table 2: Calculated Mulliken charges on the atoms of the curcumin molecule.

S. No.	Atoms	Charge	S. No.	Atoms	Charge	S. No.	Atoms	Charge
1	C	-0.745138	17	H	0.216834	33	H	0.281025
2	C	0.812092	18	H	0.195725	34	H	-0.004847
3	C	0.305395	19	C	-0.299535	35	H	0.212522
4	C	-0.345584	20	C	-0.365001	36	O	-0.297178
5	C	1.066833	21	C	0.387104	37	O	-0.296776
6	C	-1.414306	22	C	0.244085	38	O	-0.544734
7	H	0.196136	23	C	0.224704	39	H	0.541960
8	H	0.214567	24	C	-0.375295	40	C	-0.470442
9	H	0.249199	25	C	-0.166378	41	H	0.221780
10	C	-0.715274	26	O	-0.555893	42	H	0.243871
11	C	-1.477233	27	O	-0.634764	43	H	0.225977
12	C	1.133910	28	O	-0.634689	44	C	-0.470031
13	C	-0.311597	29	H	0.464871	45	H	0.244139
14	C	0.289176	30	H	0.464703	46	H	0.221945
15	C	0.844470	31	H	0.215994	47	H	0.225879
16	H	0.244782	32	H	-0.024982			

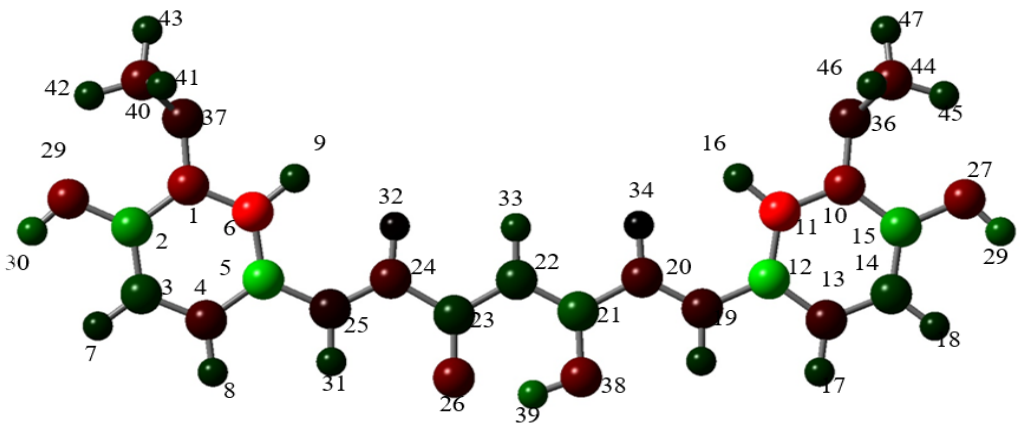

cm^{-1} and were calculated to be in the 1452 - 1420 cm^{-1} region, ideally. The highest frequency experimental bands observed in the FTIR spectrum 3079 - 3000 cm^{-1} are assigned to the aromatic C-H stretching. C-C vibrations for the aromatic and heteroaromatic compounds. The C-C symmetric stretching vibrations lie in the range between 1600 to 1400 cm^{-1} [47, 48].

C-H vibrations bands of the curcumin molecule are theoretically specified in the range 3102, 3098, 3096, 3084, 3067, 3069, 3065, 3054, 3051, 3035, 3035, 3022, 3028, 2973, 2959, 2926, and 2907 cm^{-1}. It shows good agreement with the bands observed in the calculated FTIR spectrum at 3049, 3150, 3174, 3180, 3188, 3191, 3202, 3211, 3233, and 3233 cm^{-1}. The O-H symmetric stretching vibrations are theoretically observed in between 3200 and 3650 cm^{-1}. The computed values at 3250 cm^{-1} shows good agreement with the experimental data. The C=O stretching vibration for ketones can be seen at 1740 - 1660 cm^{-1} [49]. The C-O symmetric stretching vibrations can be observed in the range from 1300 - 1000 cm^{-1} [50]. All values are well correlated to experimental results, which further validates the usability of the model.

Molecular interaction of curcumin with bacterial porins

Using the valid parameter method to dock the curcumin molecule with the proteins from *P. aeruginosa*, the best cluster's docked conformation with the lowest energy was chosen and studied. Among these porins, OccD1 and OccK1 being among the most expressed porins in *P. aeruginosa*, we have focused our studies on these two proteins [23, 25, 51, 52].

The structure OccD1, and interaction cites of curcumin in this channel is shown in figure 6. The molecule's phenolic and carbonyl functional groups, which are found on its extremities, and in the middle, respectively, can form hydrogen bonds with certain macromolecules. At the top of the channel, R190, R337, R390, and D232 formed hydrogen bonds with the phenolic and carbonyl groups of curcumin. While curcumin's phenyl rings can engage in van der Waals interactions with the side chains of aromatic amino acids. This indicates that the molecule can attach to the basic ladder of the OccD1 channel, and it can have a consecutive interaction with the ladder which may help it to slide through the constriction zone of the channel.

OccK1 has a basic ladder made up of arginine (R163, R131, R421) and lysine (K397) residues on one side and two negatively charged aspartate residues on the other side (D311 and D322) is present in the constriction region, as has been previously reported for other porins. The structure OccK1, and interaction cites of curcumin in this channel is shown in figure 7.

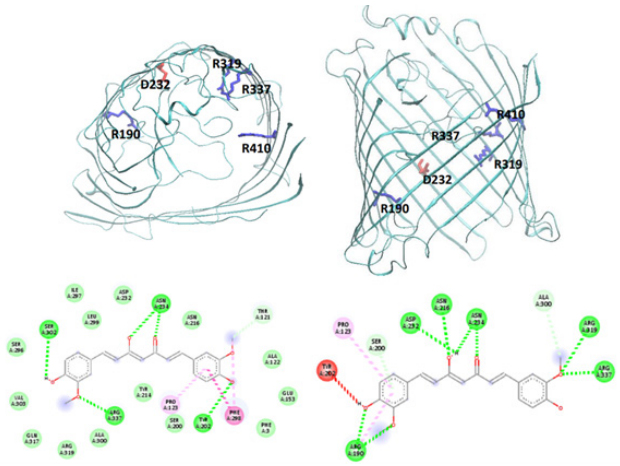

Figure 6: The structure of OccD1 protein along with important residues is shown on the top (top view on the left, side view on the right). The major interactions are shown at the bottom.

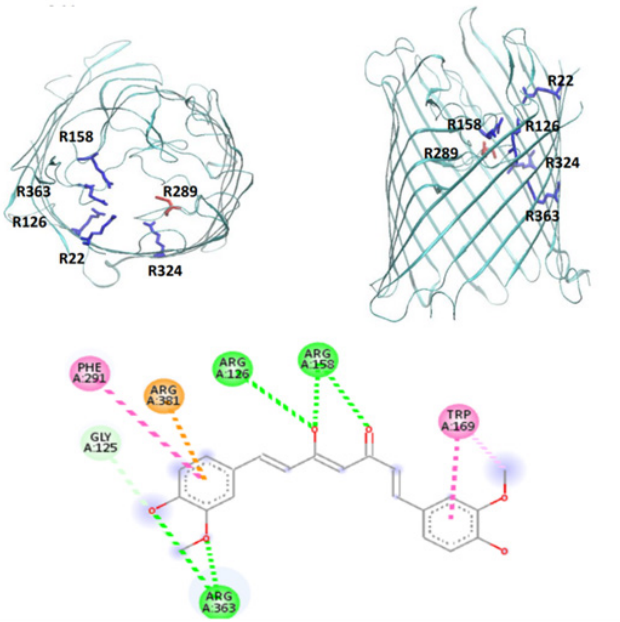

Figure 7: The structure of OccK1 protein along with important residues is shown on the top (top view on the left, side view on the right). The major interactions are shown at the bottom.

Conclusion

Here, we have analyzed the structural and spectroscopic properties of curcumin and compared them with available experimental data. We studied the HOMO-LUMO energies, ESP, and vibrational assignments (FTIR and Raman) and they agreed with available data. Molecular docking studies were done to predict the possibilities of protein OccK1 and OccD1 with curcumin. Analysis of CUR and protein revealed strong stability of the binding affinity. The docking results showed that OccD1 in the OccD family and OccK1 in the OccK family have the strongest affinity to the macromolecular targets and the lowest binding energy -8.1 and -6.7 values.

Acknowledgements

None.

Conflict of Interest

None.

References

1. Gupta SC, Prasad S, Kim JH, Patchva S, Webb LJ, et al. 2011. Multitargeting by curcumin as revealed by molecular interaction studies. *Nat Prod Rep* 28(12): 1937-1955. https://doi.org/10.1039/c1np00051a
2. Sharma RA, Gescher AJ, Steward WP. 2005. Curcumin: the story so far. *Eur J Cancer* 41(13): 1955-1968. https://doi.org/10.1016/j.ejca.2005.05.009
3. Shishodia S, Sethi G, Aggarwal BB. 2005. Curcumin: getting back to the roots. *Ann N Y Acad Sci* 1056(1): 206-217. https://doi.org/10.1196/annals.1352.010
4. Kumari V, Kumari P, Samanta S. 2021. Amphiphilic block copolymers as potential drug delivery agent for curcumin: a review. *Mater Today Proc* 43: 2944-2948. https://doi.org/10.1016/j.matpr.2021.01.299
5. Oglah MK, Mustafa YF, Bashir MK, Jasim MH, Mustafa YF. 2020. Curcumin and its derivatives: review of their biological activities. *Syst Rev Pharm* 11(3): 472-481.
6. Hsu CH, Cheng AL. 2007. Clinical Studies with Curcumin. In Aggarwal BB, Surh YJ, Shishodia S (eds) The Molecular Targets and Therapeutic Uses of Curcumin in Health and Disease. Advances in Experimental Medicine and Biology. Springer, Boston, pp 471-480.
7. Wojcik M, Krawczyk M, Wozniak LA. 2018. Antidiabetic Activity of Curcumin: Insight into its Mechanisms of Action. In Bagchi D, Nair S (eds) Nutritional and Therapeutic Interventions for Diabetes and Metabolic Syndrome. Academic Press, pp 385-401.
8. Goel A, Kunnumakkara AB, Aggarwal BB. 2008. Curcumin as "Curecumin": from kitchen to clinic. *Biochem Pharmacol* 75(4): 787-809. https://doi.org/10.1016/j.bcp.2007.08.016
9. Oglah MK, Mustafa YF, Bashir MK, Jasim MH, Mustafa YF. 2020. Curcumin and its derivatives: a review of their biological activities. *Syst Rev Pharm* 11(3): 472-481.
10. Venkatesan P, Rao MN. 2000. Structure-activity relationships for the inhibition of lipid peroxidation and the scavenging of free radicals by synthetic symmetrical curcumin analogues. *J Pharm Pharmacol* 52(9): 1123-1128. https://doi.org/10.1211/0022357001774886
11. Onoda M, Inano H. 2000. Effect of curcumin on the production of nitric oxide by cultured rat mammary gland. *Nitric Oxide* 4(5): 505-515. https://doi.org/10.1006/niox.2000.0305
12. Gorman AA, Hamblett I, Srinivasan VS, Wood PD. 1994. Curcumin-derived transients: a pulsed laser and pulse radiolysis study. *Photochem Photobiol* 59(4): 389-398. https://doi.org/10.1111/j.1751-1097.1994.tb05053.x
13. Priyadarsini KI. 1997. Free radical reactions of curcumin in membrane models. *Free Radic Biol Med* 23(6): 838-843. https://doi.org/10.1016/S0891-5849(97)00026-9
14. Priyadarsini KI, Maity DK, Naik GH, Kumar MS, Unnikrishnan MK, et al. 2003. Role of phenolic O-H and methylene hydrogen on the free radical reactions and antioxidant activity of curcumin. *Free Radic Biol Med* 35(5): 475-484. https://doi.org/10.1016/S0891-5849(03)00325-3
15. Khopde SM, Priyadarsini KI, Venkatesan P, Rao MN. 1999. Free radical scavenging ability and antioxidant efficiency of curcumin and its substituted analogue. *Biophys Chem* 80(2): 85-91. https://doi.org/10.1016/S0301-4622(99)00070-8
16. Jovanovic SV, Steenken S, Boone CW, Simic MG. 1999. H-atom transfer is a preferred antioxidant mechanism of curcumin. *J Am Chem Soc* 121(41): 9677-9681. https://doi.org/10.1021/ja991446m
17. Jovanovic SV, Boone CW, Steenken S, Trinoga M, Kaskey RB. 2001. How curcumin works preferentially with water soluble antioxidants. *J Am Chem Soc* 123(13): 3064-3068. https://doi.org/10.1021/ja003823x
18. Kolev TM, Velcheva EA, Stamboliyska BA, Spiteller M. 2005. DFT and experimental studies of the structure and vibrational spectra of curcumin. *Int J Quantum Chem* 102(6): 1069-1079. https://doi.org/10.1002/qua.20469
19. Samanta S, Roccatano D. 2013. Interaction of curcumin with PEO-PPO-PEO block copolymers: a molecular dynamics study. *J Phys Chem B* 117(11): 3250-3257. https://doi.org/10.1021/jp309476u
20. Samanta S, D'Agostino T, Ghai I, Pathania M, Gutierrez SA, et al. 2017. How to get large drugs through small pores? Exploiting the porins pathway in *Pseudomonas aeruginosa*. *Biophys J* 112(3): 416a. https://doi.org/10.1016/j.bpj.2016.11.2226
21. Samanta S, Scorciapino MA, Ceccarelli M. 2015. Molecular basis of substrate translocation through the outer membrane channel OprD of *Pseudomonas aeruginosa*. *Phys Chem Chem Phys* 17(37): 23867-23876. https://doi.org/10.1039/c5cp02844b
22. Samanta S, Bodrenko I, Acosta-Gutiérrez S, D'Agostino T, Pathania M, et al. 2018. Getting drugs through small pores: exploiting the porins pathway in *Pseudomonas aeruginosa*. *ACS Infect Dis* 4(10): 1519-1528. https://doi.org/10.1021/acsinfecdis.8b00149
23. Scorciapino MA, Acosta-Gutierrez S, Benkerrou D, D'Agostino T, Malloci G, et al. 2017. Rationalizing the permeation of polar antibiotics into Gram-negative bacteria. *J Phys Condens Matter* 29(11): 113001. https://doi.org/10.1088/1361-648X/aa543b
24. Eren E, Parkin J, Adelanwa A, Cheneke B, Movileanu L, et al. 2013. Toward understanding the outer membrane uptake of small molecules by *Pseudomonas aeruginosa*. *J Biol Chem* 288(17): 12042-12053. https://doi.org/10.1074/jbc.M113.463570
25. Liu J, Wolfe AJ, Eren E, Vijayaraghavan J, Indic M, et al. 2012. Cation selectivity is a conserved feature in the OccD subfamily of *Pseudomonas aeruginosa*. *Biochim Biophys Acta* 1818(11): 2908-2916. https://doi.org/10.1016/j.bbamem.2012.07.009
26. Liu J, Eren E, Vijayaraghavan J, Cheneke BR, Indic M, et al. 2012. OccK channels from *Pseudomonas aeruginosa* exhibit diverse single-channel electrical signatures but conserved anion selectivity. *Biochemistry* 51(11): 2319-2330. https://doi.org/10.1021/bi300066w
27. Pothula KR, Dhanasekar NN, Lamichhane U, Younas F, Pletzer D, et al. 2017. Single residue acts as gate in OccK channels. *J Phys Chem B* 121(12): 2614-2621. https://doi.org/10.1021/acs.jpcb.7b01787
28. Gutiérrez SA, Bodrenko I, Scorciapino MA, Ceccarelli M. 2016. Macroscopic electric field inside water-filled biological nanopores. *Phys Chem Chem Phys* 18(13): 8855-8864. https://doi.org/10.1039/c5cp07902k
29. Vergalli J, Bodrenko IV, Masi M, Moynié L, Acosta-Gutierrez S, et al. 2020. Porins and small-molecule translocation across the outer membrane of Gram-negative bacteria. *Nat Rev Microbiol* 18(3): 164-176. https://doi.org/10.1038/s41579-019-0294-2
30. Dennington R, Keith TA, Millam JM. 2016. Gauss View. Version 6.0.16. Semichem Inc.
31. Pagadala NS, Syed K, Tuszynski J. 2017. Software for molecular docking: a review. *Biophys Rev* 9: 91-102. https://doi.org/10.1007/s12551-016-0247-1
32. Meng XY, Zhang HX, Mezei M, Cui M. 2011. Molecular docking: a powerful approach for structure-based drug discovery. *Curr Comput Aided Drug Des* 7(2): 146-157. https://doi.org/10.2174/157340911795677602
33. Astalakshmi D. 2022. Over view on molecular docking: a powerful approach for structure based drug discovery. *Int J Pharm Sci Rev Res* 77(2): 146-157. https://doi.org/10.47583/ijpsrr.2022.v77i02.029
34. Pettersen EF, Goddard TD, Huang CC, Couch GS, Greenblatt DM, et al. 2004. UCSF Chimera - a visualization system for exploratory research and analysis. *J Comput Chem* 25(13): 1605-1612. https://doi.org/10.1002/jcc.20084
35. Humphrey W, Dalke A, Schulten K. 1996. VMD: visual molecular dynamics. *J Mol Graph* 14(1): 33-38. https://doi.org/10.1016/0263-7855(96)00018-5

36. Morris GM, Huey R, Lindstrom W, Sanner MF, Belew RK, et al. 2009. AutoDock4 and AutoDockTools4: automated docking with selective receptor flexibility. *J Comput Chem* 30(16): 2785-2791. https://doi.org/10.1002/jcc.21256

37. Pawar RP, Rohane SH. 2021. Role of autodock vina in PyRx molecular docking. *Asian J Res Chem* 14(12): 132-134.

38. Borsari M, Ferrari E, Grandi R, Saladini M. 2002. Curcuminoids as potential new iron-chelating agents: spectroscopic, polarographic and potentiometric study on their Fe(III) complexing ability. *Inorg Chim Acta* 328(1): 61-68. https://doi.org/10.1016/S0020-1693(01)00687-9

39. Lewis DF, Ioannides C, Parke DV. 1994. Interaction of a series of nitriles with the alcohol-inducible isoform of P450: computer analysis of structure—activity relationships. *Xenobiotica* 24(5): 401-408. https://doi.org/10.3109/00498259409043243

40. Karunakaran V, Balachandran V. 2012. FT-IR, FT-Raman spectra, NBO, HOMO–LUMO and thermodynamic functions of 4-chloro-3-nitrobenzaldehyde based on *ab initio* HF and DFT calculations. *Spectrochim Acta A Mol Biomol Spectrosc* 98: 229-239. https://doi.org/10.1016/j.saa.2012.08.003

41. Eakins GL, Alford JS, Tiegs BJ, Breyfogle BE, Stearman CJ. 2011. Tuning HOMO–LUMO levels: trends leading to the design of 9-fluorenone scaffolds with predictable electronic and optoelectronic properties. *J Phys Org Chem* 24(11): 1119-1128. https://doi.org/10.1002/poc.1864

42. Govindammal M, Prasath M, Kamaraj S, Muthu S, Selvapandiyan M. 2021. Exploring the molecular structure, vibrational spectroscopic, quantum chemical calculation and molecular docking studies of curcumin: a potential PI3K/AKT uptake inhibitor. *Heliyon* 7(4): E06646. https://doi.org/10.1016/j.heliyon.2021.e06646

43. Prasath M, Muthu S, Balaji RA. 2013. Vibrational spectroscopy investigation using *ab initio* and DFT vibrational analysis of 7-chloro-2-methylamino-5-phenyl-3H-1,4-benzodiazepine-4-oxide. *Spectrochim Acta A Mol Biomol Spectrosc* 113: 224-235. https://doi.org/10.1016/j.saa.2013.04.104

44. Scrocco E, Tomasi J. 1978. Electronic molecular structure, reactivity and intermolecular forces: an euristic interpretation by means of electrostatic molecular potentials. *Adv Quantum Chem* 11: 115-193. https://doi.org/10.1016/S0065-3276(08)60236-1

45. Sundius AT. 2002. Scaling of *ab initio* force fields by MOLVIB. *Vib Spectrosc* 29(1-2): 89-95. https://doi.org/10.1016/S0924-2031(01)00189-8

46. Govindammal M, Prasath M, Kamaraj S, Sathya B. 2019. *In vivo*, molecular docking, spectroscopy studies of (S)-2,3-Dihydro-5,7-dihydroxy-2(3-hydroxy-4-methoxyphenyl)-4H-1-benzopyran-4-one: a potential uptake PI3/AKT inhibitor. *Biocatal Agric Biotechnol* 18: 101086. https://doi.org/10.1016/j.bcab.2019.101086

47. Kalsi PS. 2007. Spectroscopy of Organic Compounds. New Age International, New Delhi.

48. Erdogdu Y, Unsalan OZ, Amalanathan M, Joe IH. 2010. Infrared and Raman spectra, vibrational assignment, NBO analysis and DFT calculations of 6-aminoflavone. *J Mol Struct* 980(1-3): 24-30. https://doi.org/10.1016/j.molstruc.2010.06.032

49. Huang H, Hancock RE. 1993. Genetic definition of the substrate selectivity of outer membrane porin protein OprD of *Pseudomonas aeruginosa*. *J Bacteriol* 175(24): 7793-7800. https://doi.org/10.1128/jb.175.24.7793-7800.1993

50. Köhler T, Michea-Hamzehpour M, Epp SF, Pechere JC. 1999. Carbapenem activities against *Pseudomonas aeruginosa*: respective contributions of OprD and efflux systems. *Antimicrob Agents Chemother* 43(2): 424-427. https://doi.org/10.1128/aac.43.2.424

51. Trias J, Nikaido H. 1990. Protein D2 channel of the *Pseudomonas aeruginosa* outer membrane has a binding site for basic amino acids and peptides. *J Biol Chem* 265(26): 15680-15684. https://doi.org/10.1016/S0021-9258(18)55452-1

52. Zahn M, Bhamidimarri SP, Baslé A, Winterhalter M, Van den Berg B. 2016. Structural insights into outer membrane permeability of *Acinetobacter baumannii*. *Structure* 24(2): 221-231. https://doi.org/10.1016/j.str.2015.12.009